Filling Ratio Control of TiO_2 and SiO_2 in Epoxy Composites for Permittivity-Graded Insulator with Low Coefficient of Thermal Expansion

Muneaki Kurimoto, Hiroya Ozaki and **Tooru Sawada,**
Nagoya University
Department of Electrical Engineering
Furo-cho, Chikusa-ku, Nagoya 464-8603, Japan

Takeyoshi Kato and **Toshihisa Funabashi,**
Nagoya University
Institute of Materials and Systems for Sustainability
Furo-cho, Chikusa-ku, Nagoya 464-8603, Japan

Yasuo Suzuoki
Aichi Institute of Technology
Department of Electrical and Electronics Engineering
Yakusa-cho, Toyota 470-0392, Japan

ABSTRACT

The feasibility of a permittivity-graded epoxy insulator with a low coefficient of thermal expansion (CTE) was clarified by evaluating the dielectric and thermomechanical properties of TiO_2/SiO_2 epoxy composites, which were epoxy composites co-filled with TiO_2 and SiO_2 particles. Upon varying the filling ratio of TiO_2 to SiO_2 while keeping the total filler volume constant, the relative permittivity of the TiO_2/SiO_2 epoxy composites varied in the range of 3.5-7.5 in our experiment while the CTE remained similar to that of an aluminum conductor used in gas-insulated power apparatus. The range of the relative permittivity of the TiO_2/SiO_2 epoxy composites with a low CTE satisfied the condition for realizing a permittivity-graded epoxy insulator. The application of an appropriate gradient of the permittivity distribution to a permittivity-graded epoxy insulator with a low CTE resulted in the relaxation of the electric field on the surface of an insulator.

Index Terms — **Epoxy composite, TiO_2, SiO_2, coefficient of thermal expansion (CTE), permittivity, permittivity-graded epoxy insulator**

1 INTRODUCTION

THERE has been interest in the application of permittivity-graded materials to the electrical insulators of high-voltage power apparatus [1-22]. A permittivity-graded material is a functionally graded material with an appropriate graded distribution of permittivity for relaxing the electric field stress inside and/or around the material. An epoxy insulator comprising a permittivity-graded material (permittivity-graded epoxy insulator) has been shown to have a relaxation effect on the electric field stress inside and/or around the insulator compared with a constant-permittivity epoxy insulator [1,7,13]. The electric field relaxation effect has been clarified by numerical simulation [7,9,13,16,18] and in a surface breakdown test [2-5,7,8] using insulating spacer models of gas-insulated power apparatus such as gas-insulated switchgear (GIS) and gas-insulated transmission line, potentially allowing the size-reduction of these apparatus. There is active discussion about fabrication techniques leading to the control of the permittivity distribution, which include a centrifugal force technique [3,4,6,10--12,14,15,17,19,21], lamination [2-4] and 3D printing [23].

However, several problems originating from the thermal and mechanical properties of permittivity-graded epoxy insulators have been found in practical use. A permittivity-graded epoxy insulator is made of a ceramic epoxy composite and has an appropriate density distribution of the ceramic filler to obtain a permittivity-graded distribution [3,4,7,13]. While the permittivity

Manuscript received on 10 September 2017, in final form 12 March 2018, accepted 13 March 2018. Corresponding author: M. Kurimoto.

distribution can be controlled by controlling the density distribution of a high-permittivity ceramic filler (e.g., Al_2O_3, TiO_2, $SrTiO_3$) [13,16], the coefficient of thermal expansion (CTE) distributes from high to low depending on the filler density distribution, which causes practical problems such as delamination between the insulator and metal conductor.

To obtain a permittivity-graded epoxy insulator whose CTE is as low as that of a metal conductor, we have proposed the use of an epoxy resin with a spatial distribution of the filling ratio of a high-permittivity filler to a low-permittivity filler while keeping the total filler volume constant [20,22]. In this study, the feasibility of a permittivity-graded epoxy insulator with a low CTE was clarified by evaluating the permittivity and CTE characteristics of a TiO_2/SiO_2 epoxy composite, which is an epoxy composite co-filled with TiO_2 particles as a high-permittivity filler and SiO_2 particles as a low-permittivity filler as a function of the filling ratio of TiO_2 to SiO_2. The range in the relative permittivity of the TiO_2/SiO_2 epoxy composites with a low CTE satisfied the condition for realizing a permittivity-graded epoxy insulator. The electric field relaxation effect of the permittivity-graded epoxy insulator with a low CTE was estimated by electric field analysis.

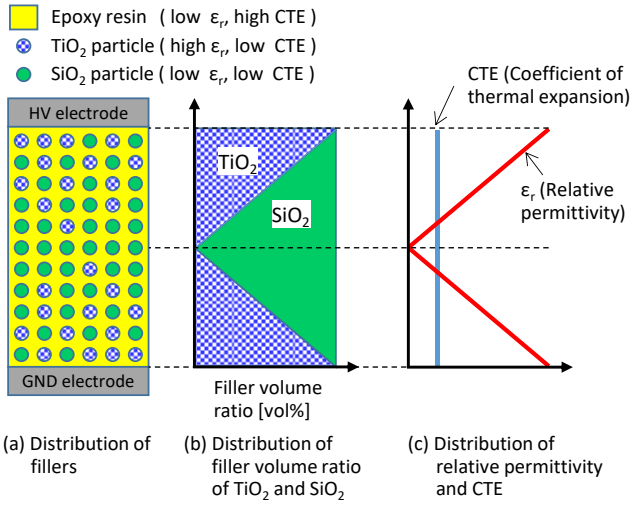

Figure 1. A conceptual diagram of a permittivity-graded epoxy insulator with a low CTE, which has a spatial distribution of the filling ratio of the high permittivity filler (TiO_2 particle) and low permittivity filler (SiO_2 particle) in epoxy resin while keeping the total filler volume constant..

2 PERMITTIVITY-GRADED EPOXY INSULATOR WITH LOW CTE

Figure 1 shows a conceptual diagram of a permittivity-graded epoxy insulator with a low CTE. Two types of ceramic filler having different permittivities are filled in the epoxy resin. The CTEs of these fillers are lower than that of the epoxy resin. To increase the permittivity of epoxy composites, a high-permittivity filler such as TiO_2 particles is used. To decrease the CTE of epoxy composites without increasing the permittivity, a low-permittivity filler such as SiO_2 particles is used. The spatial distribution of the filling ratio of TiO_2 to SiO_2 is graded in the epoxy resin while keeping the total filler volume constant. It was reported that various permittivity-graded distributions brought about relaxation of the electric field stress inside and/or around an insulator [7,9,13,16,18]. A U-shaped (or V-shaped) permittivity distribution was found to be appropriate for relaxing the electric field stress around both an upper electrode and a lower electrode [12,13], where the high-permittivity material near both the upper and lower electrode was an epoxy composite with a high volume fraction of TiO_2 and the low-permittivity material around the center of the insulator was an epoxy composite with a low volume fraction of TiO_2.

3 EXPERIMENTAL

3.1 PREPARATION OF EPOXY COMPOSITES

A TiO_2/SiO_2 epoxy composite was prepared by combining an epoxy material, TiO_2 particles and SiO_2 particles. The epoxy material was bisphenol-A epoxy resin cured with an anhydride hardener. The relative permittivity and CTE of the epoxy material were 3.4-3.5 and 70-80 ppm/K, respectively. The material of the TiO_2 particles was TiO_2 rutile crystal with a relative permittivity of 114 and a CTE of 7.1 ppm/K. The material of the SiO_2 particles was fused silica with a relative permittivity of 4 and a CTE of 0.6 ppm/K. The average diameters of the TiO_2 and SiO_2 particles were 0.6 μm and 40 μm, respectively. The silica filler size of several tens of μm makes it possible to increase the filler amount required for realizing low-expansion epoxy composite [24].

To control the relative permittivity of the TiO_2/SiO_2 epoxy composites while keeping the CTE low, the filling ratio of TiO_2 to SiO_2 was changed from 0:50 to 20:30 while maintaining a total volume fraction of 50 vol%. The total volume fraction was set to the maximum amount at which these particles were uniformly filled in this experiment. The TiO_2/SiO_2 epoxy composites with different filling ratios are denoted as, for example, TiO_2 (0%)/SiO_2(50%) and TiO_2(20%)/SiO_2(30%), where the TiO_2(0%)/SiO_2(50%) epoxy composite corresponds to the SiO_2 epoxy composite. For comparison, epoxy composites containing only TiO_2 were fabricated with the filler volume fraction of TiO_2 varied from 0 to 20 % denoted as TiO_2(0%) to TiO_2(20%), where TiO_2(0%) denotes the unfilled epoxy.

The TiO_2 and SiO_2 particles were dispersed in a mixture of bisphenol-A epoxy resin and an anhydride hardener by planetary stirring. After degassing the mixture, it was formed into sheets and bulks. These samples were then thermally cured at 60 °C for 6 h then at 100 °C for 10 h. The sheet samples used to measure the relative permittivity were 0.5 mm in thickness and 50 mm in diameter. The bulk samples used to measure the CTE were the cuboids with dimensions of 5 × 5 × 10 mm.

3.2 CHARACTERIZATION

The internal cross section of the TiO_2/SiO_2 epoxy composites was observed by field-emission scanning electron microscopy (FE-SEM) and energy dispersive X-ray spectrometry (EDX) to examine the dispersion state of the TiO_2 and SiO_2 particles in the epoxy resin.

TABLE 1. Volume fraction of filler in TiO_2/SiO_2 epoxy composites.

	Volume fraction of filler [vol%]		
	TiO_2	SiO_2	Total
TiO_2(0%) epoxy composite (denotes unfilled epoxy)	0	0	0
TiO_2(5%) epoxy composite	5	0	5
TiO_2(10%) epoxy composite	10	0	10
TiO_2(15%) epoxy composite	15	0	15
TiO_2(20%) epoxy composite	20	0	20
TiO_2(0%)SiO_2(50%) epoxy composite (denotes SiO_2 epoxy composite)	0	50	50
TiO_2(5%)SiO_2(45%) epoxy composite	5	45	
TiO_2(10%)SiO_2(40%) epoxy composite	10	40	
TiO_2(15%)SiO_2(35%) epoxy composite	15	35	
TiO_2(20%)SiO_2(30%) epoxy composite	20	30	

The capacitance and dissipation factor of each sheet sample were measured using an LCR meter after depositing an aluminum electrode (with a guard electrode) with a diameter of 40 mm on the sheet sample. The measurement frequency was from 100 Hz to 1 MHz and the measurement temperature was between 22 and 26 ℃.

The rate of increase of the length of a bulk sample (dL/L) with increasing temperature was measured using a thermomechanical analyzer. The CTE was determined from the slope of the dL/L curve. The temperature range was from 25 °C to 100 °C. Since the variation of dL/L was too large to evaluate the CTE exactly, three samples were prepared for each filling condition of the epoxy composites.

4 RESULTS AND DISCUSSION

4.1 SEM OBSERVATION OF TIO_2/SIO_2 EPOXY COMPOSITES

Figure 2 shows SEM and EDX images of the TiO_2(20%)/SiO_2(30%) epoxy composite. Green areas in Figure 2b represent Si (SiO_2) and blue areas in Figure 2c represent Ti (TiO_2). According to Figures 2a and b, SiO_2 particles with a size of 10 μm order were well dispersed in the epoxy resin. According to Figure 2c, TiO_2 particles exist among the SiO_2 particles. Figure 3 shows an enlarged SEM image of a region among SiO_2 particles. TiO_2 particles of submicrometer size were well dispersed inside the epoxy resin.

4.2 RELATIVE PERMITTIVITY

Figure 4 shows the frequency dependence of the relative permittivity of TiO_2/SiO_2 and TiO_2 epoxy composites. The relative permittivity of the TiO_2/SiO_2 epoxy composites

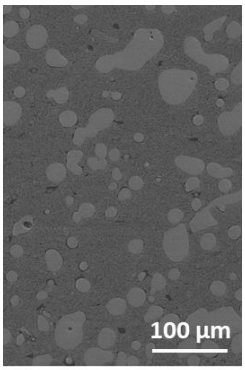

(a) SEM

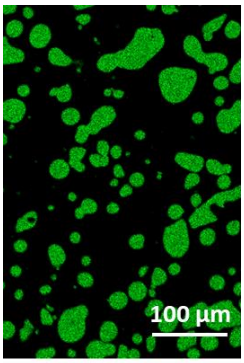

(b) EDX image of Si(SiO_2)

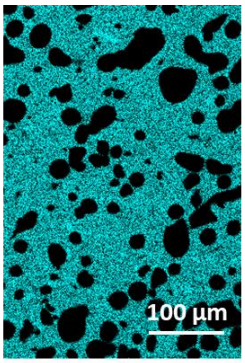

(c) EDX image of Ti(TiO_2)

Figure 2. SEM and EDX images of TiO_2(20%)/SiO_2(30%) epoxy composite. Green areas show Si(SiO_2) in (b) and blue areas show Ti(TiO_2) in (c).

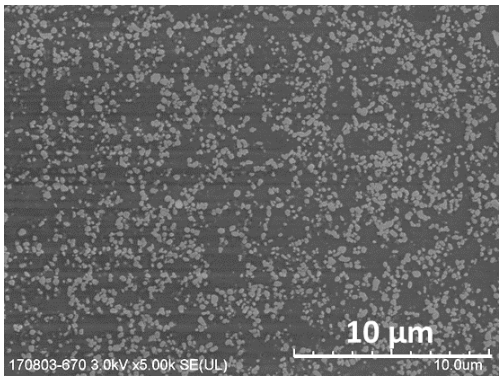

Figure 3. Enlarged SEM image of the region among SiO_2 particles in TiO_2(20%)/SiO_2(30%) epoxy composites.

increased with increasing TiO_2 filler volume and was almost the same as that of the TiO_2 epoxy composites for each filler volume of TiO_2. This is because the relative permittivity of TiO_2 particles (114) is higher than that of epoxy resin (3.5) and that of SiO_2 particles (4).

The frequency dependence of the dielectric loss tangent of the TiO_2/SiO_2 and TiO_2 epoxy composites is shown in Figure 5. No differences in the dielectric loss tangent were observed among the samples in this experiment.

The relationship between the relative permittivity at 1 MHz and the TiO_2 volume fraction is shown in Figure 6. No differences between the TiO_2/SiO_2 and TiO_2 epoxy composites

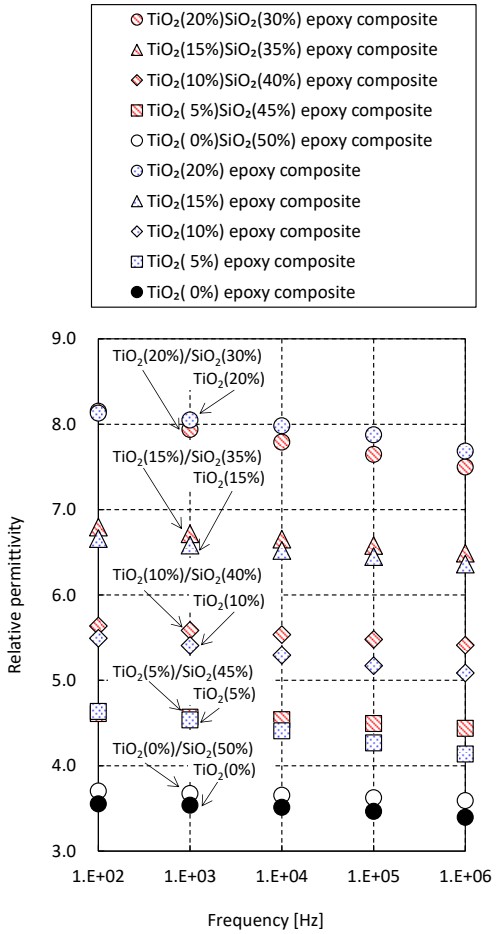

Figure 4. Frequency dependence of relative permittivity of TiO_2/SiO_2 epoxy composites, TiO_2 epoxy composites. $TiO_2(0\%)SiO_2(50\%)$ epoxy composite and $TiO_2(0\%)$ epoxy composite denote SiO_2 epoxy composite and unfilled epoxy, respectively.

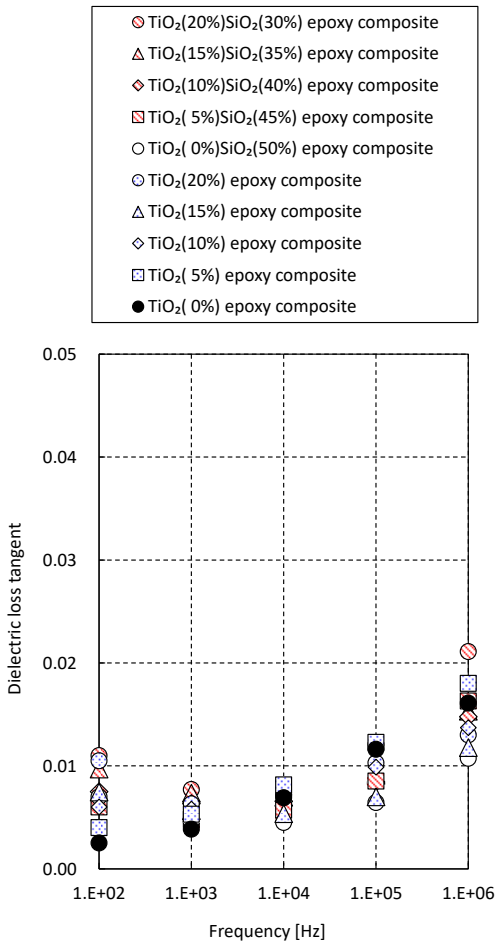

Figure 5. Frequency dependence of dielectric loss tangent of TiO_2/SiO_2 epoxy composites, TiO_2 epoxy composites. $TiO_2(0\%)SiO_2(50\%)$ epoxy composite and $TiO_2(0\%)$ epoxy composite denote SiO_2 epoxy composite and unfilled epoxy, respectively.

were observed for each filler volume. The increase in the relative permittivity of the TiO_2/SiO_2 epoxy composites was mainly caused by the increase in the TiO_2 filler volume.

To verify that the relative permittivity of the TiO_2/SiO_2 epoxy composites was reasonable, we compared the experimental data with a microstructure-based numerical model for TiO_2 epoxy composites [25]. In the model, TiO_2 particles (ε_r=114) with an average diameter of 1.18 μm were randomly placed in epoxy resin (ε_r=3.7) by three-dimensional Monte Carlo simulation. The model exhibited a range of the relative permittivities of the epoxy composites because several different configurations of TiO_2 particles with different particle positions and directions were created in the random simulations. The relative permittivity of the model was previously reported to be in good agreement with the measured permittivity of TiO_2 epoxy composites [25]. The range of the permittivities of the model is shown in figure 6. Our experimental data for the relative permittivity of TiO_2/SiO_2 epoxy composites with a TiO_2 filler volume of 10-20 vol% were in this range. However, the relative permittivity of the TiO_2/SiO_2 epoxy composites with a TiO_2 filler volume of less than 5 vol% was not in the range of the model. This may be because of the difference between the relative permittivity of the epoxy resin in our experiment (ε_r=3.4-3.5) and that in the reference (ε_r=3.7) [25]. For reference, other models in which the permittivity of two-medium composites were calculated from the volume ratio of the constituent materials and their permittivities [26] such as by Looyenga's Equation [27] and Bruggeman's Equation [28], were compared with our experimental data. Although these models did not correspond to our experimental data as they did not correspond to the experimental data for TiO_2 epoxy composites of other researchers [25], their qualitative behavior was similar to that of our data. To obtain an approximate Equation for the experimental data, Looyenga's Equation is modified in section 4.4 because this Equation is easy to modify by considering the two types of filler.

The relative permittivity of the TiO_2/SiO_2 epoxy composites increased to 7.5 upon increasing the TiO_2 filler volume to 20 vol% at a total filler volume of 50 vol%. It is possible to further increase the relative permittivity of TiO_2/SiO_2 epoxy composites by increasing the TiO_2 filler volume or by using higher-permittivity fillers together with an appropriate fabrication process for the epoxy composites by considering the filler properties such as the particle size, shape and surface conditions.

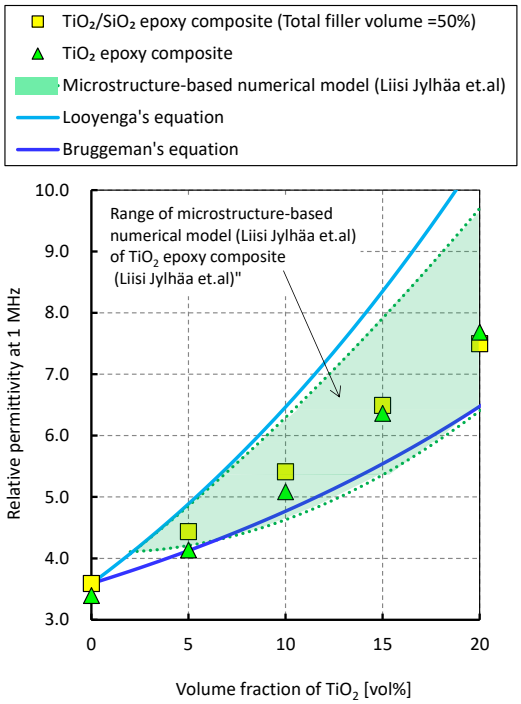

Figure 6. Relative permittivity at 1 MHz of TiO_2/SiO_2 epoxy composites and TiO_2 epoxy composites with different volume fraction of TiO_2, which are compared with relative permittivity of microstructure-based numerical model, looyenga's Equation and bruggeman's Equation.

4.3 CTE

Figure 7 shows the rate of increase of the length of bulk samples (dL/L) of the TiO_2/SiO_2 and TiO_2 epoxy composites with increasing temperature. dL/L for the TiO_2/SiO_2 epoxy composites was lower than that for the TiO_2 epoxy composites. Since the temperature increase was not stable near room temperature, the dL/L lines were slightly distorted. To calculate the coefficient of linear thermal expansion, the slope of the straight line in the temperature range of 60 to 100 °C was used.

Figure 8 shows the CTE of the TiO_2/SiO_2 and TiO_2 epoxy composites. The CTE of the TiO_2/SiO_2 epoxy composites was lower than that of the TiO_2 epoxy composites for each filler volume of TiO_2. The CTE of the TiO_2/SiO_2 epoxy composites was almost constant even for different TiO_2 volume fractions because the total volume fraction of TiO_2 and SiO_2 particles was 50 vol%.

To verify that the CTE of the TiO_2/SiO_2 epoxy composites was reasonable, we compared the CTE with the results of a calculation using a model employing the Schapery Equation (Equation (1))[22]. This Equation can be applied to epoxy composites filled with one type of particle. Here, the CTE of the TiO_2 epoxy composite whose volume fraction of TiO_2 is 50% is referred to as the upper limit of the CTE of TiO_2/SiO_2 epoxy composites and that of the SiO_2 epoxy composite whose volume fraction of SiO_2 is 50% is referred to as the lower limit of the CTE of the TiO_2/SiO_2 epoxy composites.

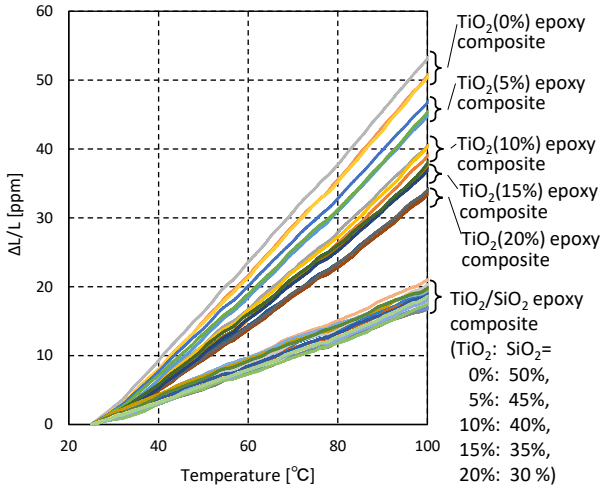

Figure 7. Rate of increase of the length of bulk samples (dL/L) of TiO_2/SiO_2 epoxy composites and TiO_2 epoxy composites with increasing temperature.

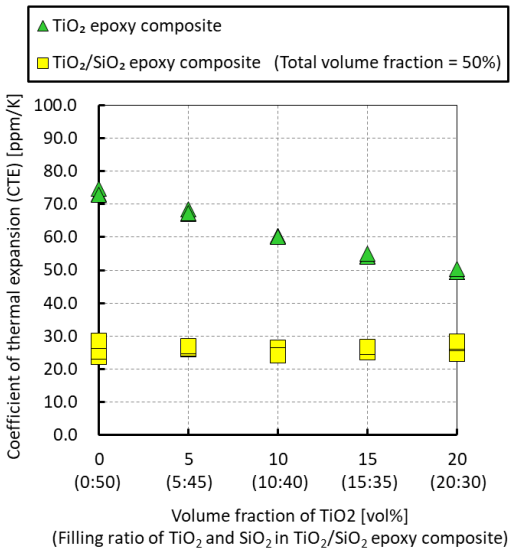

Figure 8. CTE of TiO_2/SiO_2 epoxy composites and TiO_2 epoxy composites with different volume fraction of TiO_2. TiO_2/SiO_2 epoxy composites whose filling ratio of TiO_2 and SiO_2 is 0:50 denotes SiO_2 epoxy composites with SiO_2 filler amount of 50 vol%.

$$\alpha_c = \alpha_F(V_F/100) + \alpha_E(1 - V_F/100) + \frac{\frac{1-V_F}{K_E} + \frac{V_F}{K_F} - \frac{1}{K_C}}{\frac{1}{K_E} - \frac{1}{K_F}}(\alpha_E - \alpha_F) \cdots (1)$$

Here, α_c is the CTE for the epoxy composite, α_F is the CTE for the filler (7.1 ppm/K for TiO_2 or 0.6 ppm/K for SiO_2), α_E is the CTE for the epoxy resin (74 ppm/K), V_F is the volume fraction of the filler (TiO_2 or SiO_2), K_F is the bulk modulus for the filler (141 GPa for TiO_2 or 37 GPa for SiO_2) and K_E is the bulk modulus for the epoxy resin (3.1 GPa). K_C is the bulk modulus for the epoxy composite (7.4 GPa for the TiO_2 epoxy composite or 6.4 GPa for the SiO_2 epoxy composite), which was obtained from the theoretical formula established by Hashin [30] using the moduli of the constituent materials. Figure 9 shows the CTE of the TiO_2/SiO_2 epoxy composites as a function of the TiO_2

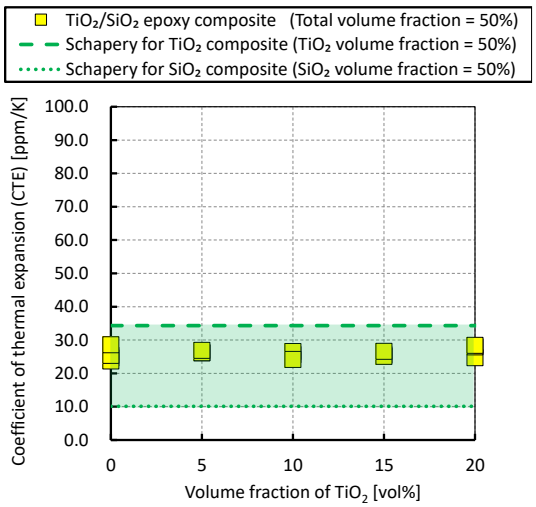

Figure 9. Comparison of CTE of TiO_2/SiO_2 epoxy composites with Schapery Equation for TiO_2 epoxy composite (TiO_2 volume fraction = 50%), SiO_2 epoxy composite (SiO_2 volume fraction = 50%.

filler volume. The CTE of the TiO_2/SiO_2 epoxy composites was in the range between the upper and lower limits of the CTE obtained from the Schapery Equation. The CTE of the TiO_2/SiO_2 epoxy composites was 23-29 ppm/K, close to that of aluminum of 24 ppm/K [24], which is used for the metal conductor in gas-insulated power apparatus. The application of a TiO_2/SiO_2 epoxy composite as an insulator inside such apparatus is expected to prevent cracks or delamination between the aluminum conductor and the insulator.

4.4 PERMITTIVITY AND CTE AS A FUNCTION OF FILLING RATIO OF TIO_2 TO SIO_2

Figure 10 shows the relative permittivity and CTE of the TiO_2/SiO_2 epoxy composites as a function of the filling ratio of TiO_2. The relative permittivity of the TiO_2/SiO_2 epoxy composites increased from 3.5 to 7.5 with increasing TiO_2 volume fraction while maintaining a low CTE. The following approximate Equation for the relative permittivity of TiO_2/SiO_2 epoxy composites was obtained by modifying Looyenga's Equation on the basis of the experimental data (Equation (2)).

$$\varepsilon_c^{1/3} = a\,(V_T/100)\varepsilon_T^{1/3} + b\,(0.5 - V_T/100)\varepsilon_S^{1/3} + c\,0.5\,\varepsilon_E^{1/3} \cdots (2)$$

where ε_c is the relative permittivity of the TiO_2/SiO_2 epoxy composite, ε_T is the relative permittivity of the TiO_2 particles (114), ε_S is the relative permittivity of the SiO_2 particles (4) and ε_E is the relative permittivity of the epoxy resin (3.5). V_T is the volume fraction of TiO_2 particles, and the total filler volume of TiO_2 and SiO_2 is 50 vol%. a is the coefficient for TiO_2 particles in the epoxy composite, b is the coefficient for SiO_2 particles in the epoxy composite and c is the coefficient for epoxy in the epoxy composite. a, b and c were determined as 0.76, 0.97 and 1.00, respectively, from the experimental data.

The following approximate Equation for the CTE of TiO_2/SiO_2 epoxy composites was obtained by modifying a linear combination Equation based on the experimental data (Equation (3)).

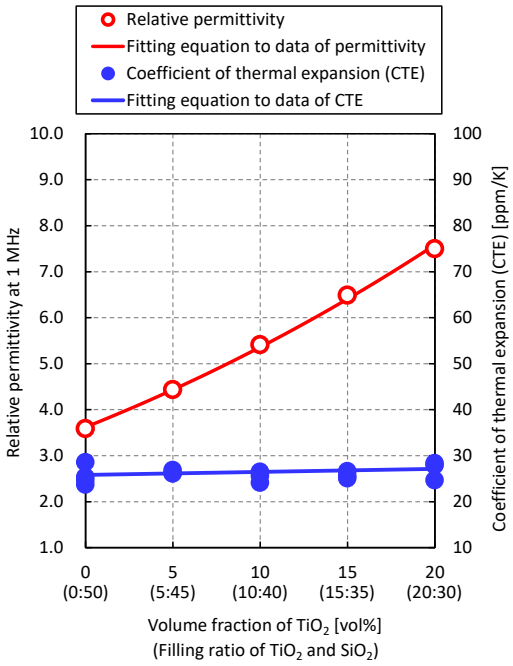

Figure 10. Estimation Equations for relative permittivity and CTE of TiO_2/SiO_2 epoxy composites based on experimental data.

$$\alpha_c = d(V_T/100)\alpha_T + e(0.5 - V_T/100)\alpha_S + f\,0.5\,\alpha_E \cdots (3)$$

where α_c is the CTE of the TiO_2/SiO_2 epoxy composite, α_T is the CTE of the TiO_2 particles (7.1 ppm/K), α_S is the CTE of the SiO_2 particles (0.6 ppm/K), α_E is the CTE of the epoxy resin (74 ppm/K). d is the coefficient for TiO_2 particles in the epoxy composite, e is the coefficient for SiO_2 particles in the epoxy composite, f is the coefficient for epoxy in the epoxy composite. d, e and f were respectively determined as 1.00, 1.00 and 0.69 to correspond to the average CTE of 26 ppm/K obtained from the experimental data.

The above investigation revealed that the relative permittivity of the fabricated TiO_2/SiO_2 epoxy composites could be changed in the range from 3.5 to 7.5 while keeping the CTE as low as 26 ppm/K on average, which was close to the CTE of the aluminum conductor in gas-insulated power apparatus.

4.5 ELECTRIC FIELD RELAXATION EFFECT OF PERMITTIVITY-GRADED EPOXY INSULATOR

To ensure that the range of the relative permittivity of the TiO_2/SiO_2 epoxy composites with a low CTE satisfied the condition for realizing a permittivity-graded epoxy insulator, the electric field relaxation effect of the permittivity-graded epoxy insulator was estimated by electric field analysis. The cylindrical spacer model used in our electric field calculation is shown in Figure 11. The model was a gas / solid composite insulation model in which a cylindrical spacer was sandwiched

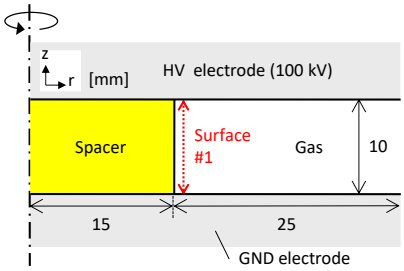

Figure 11. Calculation model for cylindrical spacer.

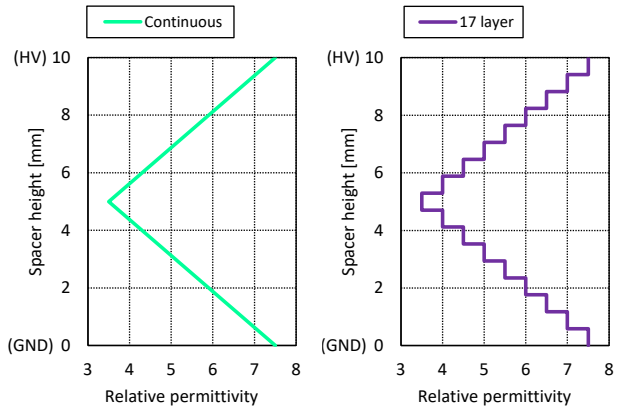

(a) Continuous permittivity-graded material

(b)17-layer permittivity-graded material

Figure 12. Permittivity distribution of permittivity-graded spacer.

between parallel plate electrodes. The voltage applied to the high-voltage electrode was 100 kV. The height of the spacer was 10 mm. COMSOL Multiphysics 4.4 was used for electric field simulation software.

To reduce the electric field strength on the upper and lower electrode surfaces, the permittivity distribution assigned to the cylindrical spacer was a V-shaped distribution with high-permittivity near the electrode and low-permittivity at the center of the spacer. To incorporate the possibility of various manufacturing methods for a permittivity-graded material, such as additive manufacturing and the centrifugal force technique, the continuous and stepwise distributions of permittivity shown in Figure 12 were applied to the spacer. The range of the permittivity distribution was set to 3.5-7.5. The stepwise distribution had 17 steps, corresponding to the case of additive manufacturing with the laminates less than 0.6-mm-thick [23].

Figure 13 shows the distributions of the electric field strength of the cylindrical spacer model with a uniform spacer (Figure 13(a)) and with a permittivity-graded material whose permittivity distribution is continuous (Figure 13(b)). The field strength was the root mean square of the electric field components in the z and r directions. The electric field distribution inside and around the spacer was controlled by the application of the permittivity-graded material.

Figure 14 shows the electric field strength along the spacer surface indicated in Figure 11 at a distance of 10 μm from the spacer surface. The electric field strength around the triple junction of the gas, electrode and spacer (TJ) was relaxed by the application of the permittivity-graded material with both the continuous distribution and the 17-step distribution. The field

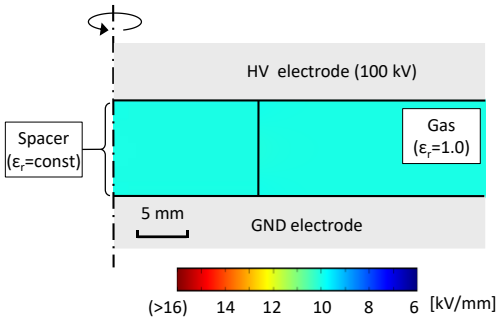

(a) Uniform permittivity material

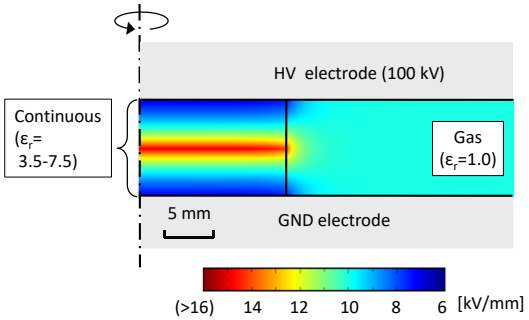

(b) Permittivity graded material with continuous distribution

Figure 13. Distribution of electric field strength of the cylindrical spacer model with uniform spacer and with permittivity graded material whose permittivity distribution is continuous.

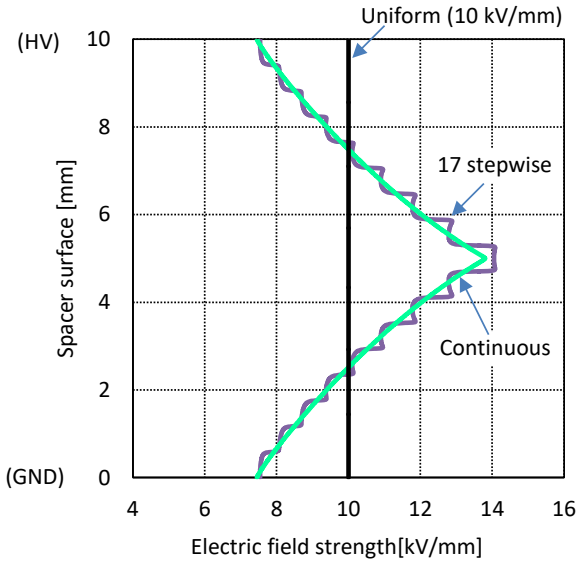

Figure 14. Electric field strength along spacer of the spacer model with uniform permittivity material, permittivity graded material whose permittivity distribution is 17 stepwise and permittivity graded material whose permittivity distribution is continuous.

relaxation effect of the permittivity-graded material was about 25%. The above results indicate that the application of a permittivity-graded epoxy insulator with an appropriate gradient of the permittivity distribution and a low CTE results

in an electric field relaxation effect on the surface of an insulator.

5 CONCLUSIONS

This study clarified the feasibility of a permittivity-graded epoxy insulator with a low CTE by evaluating the permittivity and CTE characteristics of TiO_2/SiO_2 epoxy composites. The epoxy composites with the filling ratio of TiO_2 to SiO_2 controlled from 0:50 to 20:30 while keeping the total filler volume constant exhibited a change in the relative permittivity in the range of 3.5-7.5 together with a low CTE similar to that of the aluminum conductor used in gas-insulated power apparatus. The application of a permittivity-graded epoxy insulator composed of a TiO_2/SiO_2 epoxy composite as the insulator inside such apparatus is expected to prevent cracks or delamination between the aluminum conductor and the insulator. The range of the relative permittivity of the TiO_2/SiO_2 epoxy composites with a low CTE satisfied the condition for realizing a permittivity-graded epoxy insulator. The electric field analysis revealed that the permittivity-graded epoxy insulator having a V-shaped permittivity distribution with permittivity in the range of 3.5-7.5 reduced the electric field stress around the surface of a cylindrical spacer model by up to 25%. The application of a permittivity-graded epoxy insulator with an appropriate gradient of permittivity distribution and a low CTE resulted in an electric field relaxation effect on the surface of an insulator.

To apply a permittivity-graded epoxy insulator with a low CTE to various types of insulators, it is necessary to widen the range of the permittivity distribution. This will be possible by increasing the filler volume or by using higher-permittivity particles together with an appropriate fabrication process for the epoxy composites according to the filler characteristics such as the particle size, shape and surface conditions.

ACKNOWLEDGMENT

This research work was partly supported by JSPS Grants-in-Aid for Scientific Research Grant Number JP17H04917, JP16K14213.

REFERENCES

[1] K. Kato, K. Kimura, S. Sakuma, H. Okubo: “Functionally Gradient Material (FGM) For GIS Spacer Insulation”, in *Proc. Int. Sympos. High Voltage Eng.*, 2001, vol.2, pp. 401-404.

[2] K.Kato, M.Kurimoto, K.Kimura, S.Sakuma, H.Okubo: “Experimental Study on Permittivity Graded Spacer for Control of Electric Field Distribution”, in *Proc. Int. Sympos. High Voltage Eng*., 2001, no. 4-90, pp. 549-553.

[3] M.Kurimoto, K.Kato, H.Adachi, S.Sakuma, H.Okubo: “Fabrication and Experimental Verification of Permittivity Graded Solid Spacer for GIS”, in *Annu. Rep. Conf. Electr. Insul. Dielectr. Phenom.*, 2002, pp.789-792.

[4] H.Okubo, M.Kurimoto, H.Shumiya, K.Kato, H.Adachi, S.Sakuma: "Permittivity Gradient Characteristics of GIS Solid Spacer", in *Proc. Int. Conf. on Properties and Applications of Dielectr. Materials*, 2003, S1-3.

[5] H.Shumiya, K.Kato, H.Okubo: “Feasibility Study on FGM (Functionally Graded Materials) Application for Gas Insulated Equipment”, in *Annu. Rep. Conf. Electr. Insul. Dielectr. Phenom.*, 2004, 5A-6.

[6] H.Shumiya, K.Kato, H.Okubo: “Fabrication and Prediction Techniques for FGM (Functionally Graded Materials) Application to Solid Insulators”, in *Annu. Rep. Conf. Electr. Insul. Dielectr. Phenom.*, 2005, 5A-6.

[7] K.Kato, M.Kurimoto, H.Shumiya, H.Adachi, S.Sakuma, H.Okubo: “Application of Functionally Graded Material for Solid Insulator in Gaseous Insulation System”, IEEE Trans. Dielectr. Electr. Insul., vol.13, no. 1, pp. 362-372, 2006.

[8] H.Okubo, H.Shumiya, M.Ito, K.Kato: “Insulation Performance of Permittivity Graded FGM (Functionally Graded Materials) in SF6 Gas under Lightning Impulse Conditions”, in *Proc. IEEE Int. Sympos. Electr. Insul*., 2006, pp. 332-335.

[9] H.Okubo, H.Shumiya, M.Ito, K.Kato: “Optimization Techniques on Permittivity Distribution in Permittivity Graded Solid Insulators”, in *Proc. IEEE Int. Sympos. Electr. Insul.,* 2006, pp. 519-522.

[10] N.Hayashi, T.Sugahara, S.Tsuru, M.Hara, “Improved Method to Simulate Gradient in Alumina Packing Fraction in Alumina/Epoxy Composite Fabricated by a Centrifugal Method”, IEEJ Trans. Electr. Electronic Eng., vol. 1, no. 2, pp. 194-206, 2006.

[11] N.Hayashi, T.Sugahara, M.Hara, “Numerical Simulation of a Centrifugal Process Involved in a Fabrication of Functionally Graded Material from an Alumina/Epoxy Mixture”, in *Proc. Int. Sympos. High Voltage Eng.*, 2007, no. T4-384.

[12] M.Kurimoto, A.Kai, K.Kato, H.Okubo: “Fabrication of Permittivity Graded Materials for Reducing Electrid Stress on Electrode Surface” in *Proc. IEEE Int. Sympos. Electr. Insul*., 2008, pp. 265-268.

[13] M.Kurimoto, K.Kato, M.Hanai, Y.Hoshina, M.Takei, H.Okubo: “Application of Functionally Graded Material for Reducing Electric Field on Electrode and Spacer Interface”, IEEE Trans. Dielectr. Electr. Insul., vol.17, no.1, pp. 256-263, 2010.

[14] J.Shimomura, Y.Fujii, N.Hayakawa, M.Hanai, H.Okubo, “Fabrication Technique of Permittivity Graded Materials Using Particle Movement Simulation”, in *Annu. Rep. IEEE Conf. Electr. Insul. Dielectr. Phenom*., 2010.

[15] H.Okubo, J.Shimomura, Y.Fujii, N.Hayakawa, M.Hanai, K.Kato, “Fabrication and Simulation Techniques of Permittivity Graded Materials for Gas Insulated Power Equipment”, in *Proc. Int. Sympos. High Voltage Eng.*, 2011, E-095.

[16] H.Ju, B.Kim, K.Ko: “Optimal Design of an Elliptically Graded Permittivity Spacer Configuration in Gas Insulated Switchgear”, IEEE Trans. Dielectr. Electr. Insul., vol.18, no.4, pp. 1268-1273, 2011.

[17] N.Hayakawa, J.Shimomura, T.Nakano, M.Hanai, K.Kato, H.Okubo, “Fabrication Technique of Permittivity Graded Materials (FGM) for Disk-Type Solid Insulator”, in *Annu. Rep. IEEE Conf. Electr. Insul. Dielectr. Phenom.*, 2012, pp. 32-35.

[18] H.Ju, B.Kim, K.Ko: “Optimization of a Grounded Electrode Shape in Gas Insulated Switchgear with a Reversely Elliptical Permittivity Graded Insulator”, IEEE Trans. Dielectr. Electr. Insul., vol. 20, no.5, pp.1749-1754, 2013.

[19] J.Ishiguro, M.Kurimoto, H.Kojima, K.Kato, H.Okubo, N.Hayakawa: “Electric Field Control in Coaxial Disk-Type Solid Insulator by Functionally Graded Materials (FGM)” in *Annu. Rep. IEEE Conf. Electr. Insul. Dielectr. Phenom.*, 2014, pp. 663-666.

[20] H.Ozaki, M.Kurimoto, T.Kato, T.Funabashi, Y.Suzuoki : “Study on filler distribution in two-ceramic permittivity-graded epoxy composite with constant thermal-expansion coefficient”, in *Proc. 46th Sympos. Electr. Electron. Insul. Mat. Appl. Sys.*, 2015, no. MVP-11, pp. 223‐224.

[21] N.Hayakawa, J.Ishiguro, H.Kojima, K.Kato, H.Okubo: “Fabrication and simulation of permittivity graded materials for electric field grading of gas insulated power apparatus”, IEEE Trans. Dielectr. Electr. Insul., vol. 16, no.1, pp. 547-554, 2016.

[22] H. Ozaki, M. Kurimoto, T. Sawada, T. Kato, T. Funabashi, Y. Suzuoki , “Evaluation of Coefficient of Thermal Expansion and Relative Permittivity of TiO2/SiO2 Epoxy Composite”, in *Int. Sympos. Electr. Insul. Materials*, accepted 2017.

[23] M.Kurimoto, H.Ozaki, Y.Yamashita, T.Funabashi, T.Kato, Y.Suzuoki:” Dielectric Properties and 3D Printing of UV-cured Acrylic Composite with Alumina Microfiller”, IEEE Trans. Dielectr. Electr. Insul., vol. 23, no. 5, pp. 2985-2992, 2016.

[24] T. Imai, F. Sawa, T. Nakano, T. Ozaki, T. Shimizu, M. Kozako, T. Tanaka, “Effects of Nano- and Micro-filler Mixture on Electrical Insulation

Properties of Epoxy Based Composites", IEEE Trans. Dielectr. Electr. Insul., vol. 13, No. 2, pp. 319-326, 2006.

[25] L. Jylhä, J. Honkamo, H. Jantunen, A. Sihvola, "Microstructure-based numerical modeling method for effective permittivity of ceramic/polymer composites", J. Appl. Phys., 97, 104104(2005)

[26] Gorur G.Raju, *Dielectrics in Electric Fields*, Marcel dekker, Inc., pp.77-90, 2003.

[27] H.Looyenga "Dielectric constants of heterogeneous mixtures" Physica,vol. 31, pp. 401-406, 1965.

[28] D.A.G. Bruggeman An. Physik, 24, p. 636, 1935.

[29] R.A.Schapery:" Thermal Expansion Coefficients of Composite Materials Based on Energy Principles", J. Composite Materials, vol.2, no. 3, pp. 380-303, 1968.

[30] Z.Hashin, S.Shtrikman: " A variational approach to the theory of the elastic behaviour of multiphase materials" , J. Mechanics and Physics of Solids, vol.11, no.2, pp.127-140, 1963.

Muneaki Kurimoto (M'10) was born in 1978. He received the B.Sc. degree in 2001, the M.S. degree in 2003 and the Doctor of Eng. degree in 2010, all in electrical engineering, from Nagoya University, Japan. From 2003 to 2007, he joined Aisin Seiki Corporation, Japan. From 2010 to 2013, he was an Assistant Professor at Toyohashi University of Technology, Japan. Since 2013, he has been an Assistant Professor at Nagoya University. He is a member of IEE of Japan and IEEE.

Hiroya Ozaki was born in 1992. He received the B.Sc. degree in 2014, the M.S. degree in 2016 in electrical engineering from Nagoya University, Nagoya, Japan. From 2016, he joins Cannon in, Japan. He is a member of IEE of Japan and IEEE.

.

Tooru Sawada was born in 1994. He received the B.Sc. degree in electrical engineering in 2016 from Nagoya University, Nagoya, Japan. Since 2017, he is a M.S. degree student in electrical engineering at Nagoya University. He is a student member of IEE of Japan.

Takeyoshi Kato (M'09) was born in 1968. He received the B.Sc. degree in 1991, the M.S. degree in 1993 and the Doctor of Eng. degree in 1996, all in electrical engineering, from Nagoya University, Japan. From 1996 to 2015, he was on the faculty of Nagoya University, Japan. Since 2015, he has been a Professor at Nagoya University. He is a member of IEE of Japan and IEEE.

Toshihisa Funabashi (M'90-SM'96) was born in Aichi, Japan in 1951. He received the B.S. degree from Nagoya University, Japan, in 1975, and the Ph.D. degree from Doshisha University, Kyoto, Japan, in 2000, both in electrical engineering. From 1975 to 2014, he joined Power System Engineering Division, Meidensha Corporation, Tokyo, Japan. Since 2014, he has been a Professor at Nagoya University. He is a member of IEE of Japan, IET and IEEE.

Yasuo Suzuoki (M'94) was born in 1950. He received the B.S. degree in 1973, the M.S. degree in 1975 and the Doctor of Eng. degree in 1978, all in electrical engineering, from Nagoya University, Nagoya, Japan. From 1978 to 1995, he was on the faculty of Nagoya University. From 1995 to 2016, he was a Professor at Nagoya University. At present, he is a Professor at Aichi Institute of Technology. He is a member of IEE of Japan and IEEE.